Automatic Generation of Subdomain Models in 2-D FDTD Using Reduced Order Modeling

Bart Denecker, Frank Olyslager, Luc Knockaert, and Daniël De Zutter

***Abstract*—A new method combining a finite difference method and a reduced order model (ROM) algorithm is presented for two-dimensional (2-D) electromagnetic problems. The problem space is subdivided into subdomains of a generic type. By discretizing the spatial derivatives in a way similar to the finite-difference in time-domain technique (FDTD), the state equations are written down in each subdomain. From that, an FDTD-subdomain model is derived. Finally, the different subdomains are reconnected and the original problem is solved by a leapfrog time-stepping algorithm. Some numerical results are presented to illustrate the new approach.**

***Index Terms*—FDTD, Laguerre approximants, reduced order modeling.**

I. INTRODUCTION

THE finite-difference time-domain method (FDTD) is a general method for analyzing electromagnetic problems. The main problem that arises is the huge amount of state variables that is being generated, certainly when electrically small objects have to be modeled. Recently, some interesting results have been put forward by combining FDTD and reduced order modeling (ROM). Typically, the frequency response is approximated by its Padé approximant using the Lanczos algorithm. In [1] and [2], fast calculation is ensured by avoiding LU-decomposition. This only leads to good results at high frequencies (early times) but fails to give a reliable model at lower frequencies. In [3], overall good results were obtained but with high computational costs. In this letter, we subdivide the simulation space in subdomains and generate a reduced model for each domain, using a Laguerre approximant. The different ROM's of the subdomains are then connected and iterated in an FDTD fashion. One could say that each ROM for a subdomain is an automatic generation of a subcell model as was obtained in a nonautomatic fashion, e.g., for a thin wire [4]. In this letter, we use a new ROM scheme which has the advantage also to be stable at late times i.e., for the lower frequencies. A detailed description can be found in [5] and [6] and will not be repeated here.

II. A SUBDOMAIN APPROACH

Assuming a two-dimensional (2-D) electromagnetic problem, let us consider the TE case, and no variation in the z-direction. Spatially discretizing a part of this region (Fig. 1),

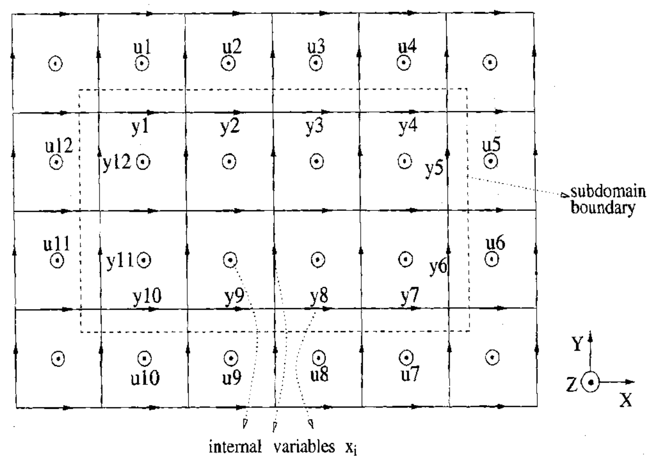

Fig. 1. Two-dimensional grid and the location of $\mathbf{u}$ and $\mathbf{y}$ variables.

as in FDTD [4], permits us to write the time-domain differential equations for every field component as

$$\mathbf{C}\dot{\mathbf{x}} = -\mathbf{G}\mathbf{x} + \mathbf{B}\mathbf{u}; \quad \mathbf{y} = \mathbf{L}^T\mathbf{x}. \tag{1}$$

In these expressions, $\mathbf{x}$ is a vector of dimension N that holds every field component of that region (E_x, E_y and H_z), $\mathbf{u}$ is a vector of dimension p that holds the field components H_z at the boundary of the domain and $\mathbf{y}$, also of dimension p, holds the E_x and E_y field components at the boundary. $\mathbf{u}$ can be seen as the sources of the fields inside the subdomain and $\mathbf{y}$ are the observation variables. In this way a generalization of the E-field update equation in FDTD is obtained. Remark however that the role of $\mathbf{u}$ and $\mathbf{y}$ can be interchanged to obtain a generalization of the H-field update equation. In Fig. 1, the elements of $\mathbf{u}$ and $\mathbf{y}$ are shown. The matrices $\mathbf{C}$ and $\mathbf{G}$ are of dimension $N \times N$, $\mathbf{B}$ and $\mathbf{L}$ are of dimension $N \times p$. All these matrices are very sparse. The original 2-D grid can be divided into this kind of subdomains where neighboring subdomains interact through $\mathbf{u}$ and $\mathbf{y}$. If now, the subdomain borders are taken far away from the discontinuities, the number of field components needed to model the field behavior at these borders can be taken smaller. The original u_i $(i = 1 \ldots p)$, can then be mapped to fewer u'_i $(i = 1 \ldots p')$ and similar for y_i. In this way one can use a fine mesh inside a subdomain and connect it to a coarser mesh at the outside. The matrices $\mathbf{B}$ and $\mathbf{L}$ have to be adjusted accordingly. A special case arises when the field components at each border are replaced by a single one, then the average is taken across each border. Since only a small portion of the variables is of interest to us, namely, the variables in $\mathbf{y}$ together with the variables in $\mathbf{u}$, it gives us the opportunity to apply a new model

Manuscript received April 5, 2000; revised June 8, 2000.
The authors are with the Department of Information Technology (INTEC), Ghent University, B-9000 Gent, Belgium (e-mail: bart.denecker@intec.rug.ac.be).
Publisher Item Identifier S 1051-8207(00)07047-1.

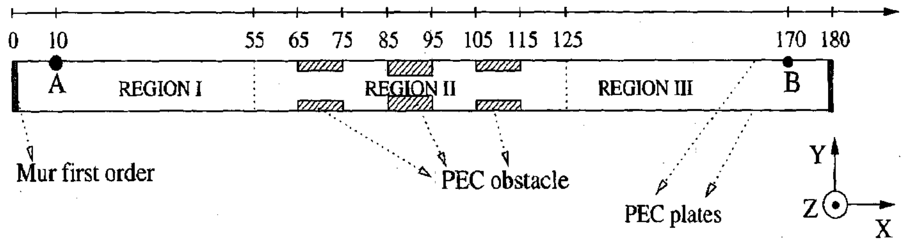

Fig. 2. TEM simulation problem.

order reduction method [5], [6] to reduce the number of variables N to pq, where q is the order of reduction. The method is based on an expansion of the impulse response in terms of scaled Laguerre functions $\sqrt{2\alpha}e^{-\alpha t}l_n(2\alpha t)$ $(n = 0, 1, \ldots)$ [7]. In [5] $\alpha = 2\pi f_{\max}$ is put forward as a good choice with $f_{\max}$ the maximum frequency of interest. The reduced system representation of (1) is

$$\hat{\mathbf{C}}\dot{\mathbf{z}} = -\hat{\mathbf{G}}\mathbf{z} + \hat{\mathbf{B}}\mathbf{u}; \quad \mathbf{y} = \hat{\mathbf{L}}^T\mathbf{z}. \tag{2}$$

The vectors $\mathbf{u}$ and $\mathbf{y}$ remain unchanged, but the vector $\mathbf{x}$ (dimension N) has been replaced by $\mathbf{z}$ (dimension pq). By choosing q, the frequency region over which the new system approaches the original system can be changed. The matrices $\hat{\mathbf{G}}$, $\hat{\mathbf{C}}$, $\hat{\mathbf{B}}$ and $\hat{\mathbf{L}}$ are now dense matrices. Discretizing time in (2) gives

$$\mathbf{z}^{n+1} = \left(\frac{\hat{\mathbf{C}}}{\Delta_t} + \frac{\hat{\mathbf{G}}}{2}\right)^{-1}\left(\frac{\hat{\mathbf{C}}}{\Delta_t} - \frac{\hat{\mathbf{G}}}{2}\right)\mathbf{z}^n + \left(\frac{\hat{\mathbf{C}}}{\Delta_t} + \frac{\hat{\mathbf{G}}}{2}\right)^{-1}\hat{\mathbf{B}}\mathbf{u}^{n+\frac{1}{2}} \tag{3}$$

$$\mathbf{y}^{n+1} = \hat{\mathbf{L}}^T\mathbf{z}^{n+1}. \tag{4}$$

Similar to the FDTD-method [4], a leapfrog time-stepping algorithm can be used to combine different subdomains. This means that if a subdomain is updated at $t = n\Delta_t$, the neighboring subdomains are updated at $t = (n + 1/2)\Delta_t$. An efficient algorithm is thus obtained, without requiring any interpolations or extrapolations. Making sure that the subdomains have a generic appearance no new reduction has to be performed every time the same subdomain is being reused. In that way, a library of subdomain components or automatic subcell models can be generated that can be used in different FDTD simulations. If locally in an FDTD problem a fine mesh is needed to model a small structure one can generate a ROM based on the fine mesh for a subdomain enclosing the structure and then connect it to the coarse FDTD mesh at the outside.

III. Numerical Results

We study the reflection and transmission coefficient of a parallel-plate waveguide problem, with a metallic object causing reflection (Fig. 2). The infinite waveguide was modeled by a 63 cm waveguide terminated in Mur first order absorbing boundary conditions. The distance between the plates is 3.15 cm and the waveguide is filled with air but with very

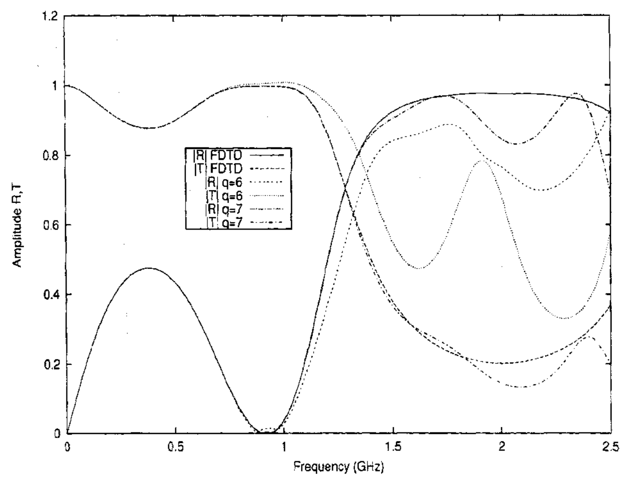

Fig. 3. Numerical results for waveguide with single obstacle and $f_{\max} = 0.25$ GHz.

small losses added ($\sigma = 0.000\,025$ S/m) to ensure stability of the ROM algorithm. This has no significant effect on the results. The TEM-mode is the only propagating mode, the first higher mode only propagates for $f > 4.76$ GHz. The number of cells is $n_x = 180$ and $n_y = 9$ and the size of the cells is $\Delta_x = \Delta_y = \Delta = 3.5$ mm. In the waveguide there are three metallic irises (Fig. 2). The excitation of the problem is a current injected at $x = 10\Delta$ (A on Fig. 2). The reflected field is recorded at the same location, the transmitted field is recorded at $x = 170\Delta$ (B on Fig. 2).

For our method, the computational domain is divided into three regions, at cell 55 and at cell 125, as shown in Fig. 2. There are only contributions to $\mathbf{u}$ and $\mathbf{y}$ for each subdomain at the left and right sides of these domains. The nine variables in $\mathbf{u}$ and $\mathbf{y}$ at each side are replaced by the average of these field variables and then connected. In other words, we have $p = 2$ for each region. Physically, this means that we characterize each subregion at its boundaries by equivalent voltages and currents associated with the TEM-mode. Different regions interact through this TEM-mode. In region I and III, there is an extra $\mathbf{u}$-component for the current source (in region III this source is zero) and an extra $\mathbf{y}$-component for the recording of the fields. The reduction factor q is selected to be identical for every region ($q_{\mathrm{I}} = q_{\mathrm{II}} = q_{\mathrm{III}}$). Although it is possible to select a considerably larger time step in the reduced model, for reasons of comparison, this time step is taken to be the same as for FDTD. In Fig. 3, our results (with $f_{\max} = 0.25$ GHz) are compared

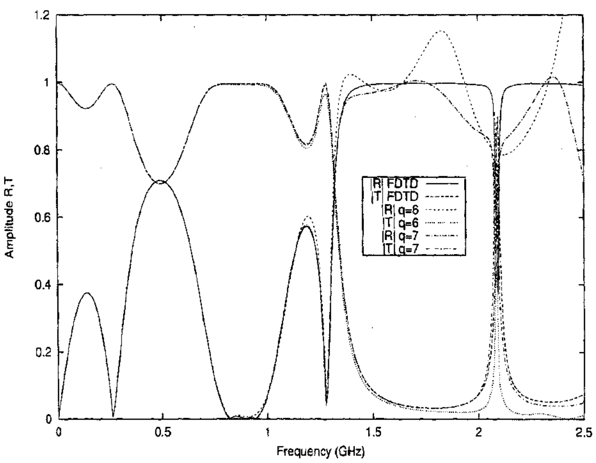

Fig. 4. Numerical results for waveguide with twice the obstacle and $f_{\max} = 0.25$ GHz.

with FDTD-results in the fine mesh without any reduction. The figure shows the amplitude of the TEM-mode reflection (at A) and transmission coefficient (at B). The time step in the full FDTD and the ROM technique are equal to the Courant limit of the full fine mesh FDTD, i.e., $\Delta_t = 8.24\,10^{-12}$s. Up to a reduction factor of $q = 7$ there is a very good agreement, even for $q = 6$ the results are very acceptable for $f < 0.75$ GHz, larger than $f_{\max}$. Although not shown here, it appears that for larger q the frequency domain where the results coincide grows without increasing $f_{\max}$. The amount of FLOP's needed in the full FDTD is about ten times larger than in the reduced technique. Of course this assumes that the ROM and the matrices in (3) and (4) are calculated in advance. The CPU time requirements can be reduced further by using a larger time step in the reduced technique. Numerical experiments indicate, at least in our example, that the timestep can be as large as five times the Courant limit. The memory requirements are reduced by a factor 100. Since the reduction algorithm itself is computationally expensive, reusing the ROM is important. This possibility is validated by another simulation. As in the previous problem (Fig. 2), the regions I and III remain the same, but the region II is inserted twice. Fig. 4 makes it clear that the several subdomains and their ROM can be combined again, leading to a very efficient modeling algorithm. Finally, the effect of changing $f_{\max}$ and q was investigated numerically. Even for $f_{\max}$ as small as 0.05 GHz the mean overall error for $f \leq 1.5$ GHz is larger than 3.9% for $q = 6$, reaching 20% for $f_{\max} = 1$ GHz, $q = 6$. For $q = 7.$, however, the error remains below 2% for $f < 1.5$ GHz and for 0.05 GHz $< f_{\max} < 1$ GHz. Theoretical understanding is still lacking.

References

[1] R. F. Remis and P. M. van den Berg, "A modified Lanczos algorithm for the computation of transient electromagnetic wavefields," *IEEE Trans. Microwave Theory Tech.*, vol. 45, pp. 2139–2149, Dec. 1997.

[2] A. C. Cangellaris and L. Zhao, "Rapid FDTD simulation without time stepping," *IEEE Microwave Guided Wave Lett.*, vol. 9, pp. 4–6, Jan. 1999.

[3] L. Zhao and A. C. Cangellaris, "Reduced-order modeling of electromagnetic field interactions in unbounded domains truncated by perfectly matched layers," *Microwave Opt. Technol. Lett.*, vol. 17, pp. 62–66, Jan. 1998.

[4] A. Taflove, *Computational Electrodynamics: The Finite-Difference Time-Domain Method*. Norwood, MA: Artech House, 1995.

[5] L. Knockaert and D. De Zutter, "Passive reduced order multiport modeling: The Padé-Laguerre, Krylov-Arnoldi-SVD connection," *AEÜ Int. J. Electron. Commun.*, vol. 53, no. 5, pp. 254–260, 1999.

[6] ——, Laguerre-SVD reduced order modeling, in *IEEE Trans. Microwave Theory Tech.*, to be published.

[7] Z. Zang, A. Cantoni, and K. L. Teo, "Continuous-time envelope-constrained filter design via Laguerre filters and $\mathcal{H}_\infty$ optimization methods," *IEEE Trans. Signal Processing*, vol. 46, pp. 2601–2610, Oct. 1998.